Distribution Agreement

In presenting this thesis as a partial fulfillment of the requirements for a degree from Emory University, I hereby grant to Emory University and its agents the non-exclusive license to archive, make accessible, and display my thesis in whole or in part in all forms of media, now or hereafter known, including display on the world wide web. I understand that I may select some access restrictions as part of the online submission of this thesis. I retain all ownership rights to the copyright of the thesis. I also retain the right to use in future works (such as articles or books) all or part of this thesis.

Signature:

_____	_____
Emily Grossniklaus	04/25/2010

Studies of Vesicle Trafficking Following Functional Depletion of Clathrin: Use of Clathrin Light Chain-FKBP-Binding Domain Chimera

By

Emily Grossniklaus

Adviser: Victor Faundez, MD, PhD

Department of Biology

Victor Faundez, MD, PhD
Adviser

Steven L'Hernault, PhD
Committee Member

Winfield Sale, PhD
Committee Member

Rachelle Spell, PhD
Committee Member

04/25/2010

Studies of Vesicle Trafficking Following Functional Depletion of Clathrin: Use of Clathrin Light Chain-FKBP-Binding Domain Chimera

By

Emily Grossniklaus

Adviser: Victor Faundez, MD, PhD

An abstract of
A thesis submitted to the Faculty of Emory College of Arts and Sciences
of Emory University in partial fulfillment
of the requirements of the degree of
Bachelors of Sciences with Honors

Department of Biology

2010

Abstract

Studies of Vesicle Trafficking Following Functional Depletion of Clathrin:
Use of Clathrin Light Chain-FKBP-Binding Domain Chimera
By Emily Grossniklaus

Eukaryotic cells use vesicle carriers to target and transfer membrane proteins between selected intracellular compartments in a process that is generally referred to as vesicle trafficking. The clathrin triskelion molecule plays a critical role during vesicle trafficking, as it coats vesicles early in formation and recruits molecular machinery to help pinch the coated pits off from the plasma membrane, creating a fully formed and mature vesicle. A host of adaptor proteins work together with clathrin, interacting with membrane-bound proteins to create sites of high protein concentration that attract clathrin and initiate vesicle formation. Due to the precise and specific nature of adaptor protein interactions with membrane-bound receptors, adaptor proteins are largely responsible for determining the final protein composition of each vesicle.

An outstanding question is how the single protein clathrin regulates specific vesicle formation and composition in concert with these adaptor proteins. It is generally accepted that the AP-1 and AP-2 adaptor proteins require interaction with the clathrin triskelion for successful vesicle formation, but less is known about the role of AP-3 in vesicle biogenesis pathways. In my project, I have tested the hypothesis that AP-3 participates in alternative trafficking pathways that do not require functional clathrin. Clathrin function was perturbed using a recombinant clathrin light chain containing a modified FKBP domain that is susceptible to oligomerization following treatment by the drug AP20187. This recombinant clathrin molecule was expressed in mammalian cell lines in culture and rendered non-functional by AP20187 prior to subcellular fractionation and immunofluorescent microscopy experiments. I observed that the affects of clathrin disruption on AP-3 concentration in clathrin coated vesicle fractions was unique from the affects of clathrin on AP-1 and AP-2. This finding contrasts with the current notion that all clathrin-adaptor interactions are mechanistically similar. Rather, this data supports an alternative hypothesis that the kinetics of AP-3 interactions of clathrin are slower than those of clathrin with AP-1 and AP-2, or that AP-3 participates in clathrin-independent trafficking pathways.

Studies of Vesicle Trafficking Following Functional Depletion of Clathrin: Use of Clathrin Light Chain-FKBP-Binding Domain Chimera

By

Emily Grossniklaus

Adviser: Victor Faundez, MD, PhD

A thesis submitted to the Faculty of Emory College of Arts and Sciences
of Emory University in partial fulfillment
of the requirements of the degree of
Bachelors of Sciences with Honors

Department of Biology

2010

TABLE OF CONTENTS

LIST OF TABLES AND FIGURES

Introduction

A. The Discovery of Clathrin and its Proposed Role in Coat Formation

Clathrin coated vesicles (CCVs) were first identified via electron microscopy by Roth and Porter, who described the process of vesicle formation and identified coated pits as vesicle precursors [13] [**Figure 1**]. CCVs were first isolated by Kanaseki and Kadota [14] through a procedure that was later refined by Pearse [2]. Through this procedure, Pearse was able to purify and examine coat proteins obtained from brain, adrenal medulla, and lymphoma cell lines. Although derived from different cell types, these coat proteins were found to be identical by a one-dimensional peptide fragment analysis. Amino acid sequencing revealed that this coat protein, clathrin, was highly conserved across species and cell types. The conservation of clathrin lent strong support to Pearse's initial hypothesis that clathrin coated vesicles guide membrane transport throughout the cell [1]. Genetic analysis in *Drosophila* and *C.elegans* has provided definitive evidence for the role of clathrin in vesicle formation [3-5].

B. Stepwise Mechanism of Vesicle Formation and Generalized Trafficking Pathway

Clathrin coated vesicles are formed at the plasma membrane and in various intracellular compartments according to the following mechanistic steps. To begin, membrane-bound receptor protein and soluble luminal enzymes with specific sorting signals localize into coated pits. These pits bud into the cytoplasm, recruiting adaptor proteins (APs) and clathrin triskelions to form an exterior coat before pinching off from the plasma membrane of the donor organelle and becoming fully formed vesicles [**Figure 2**] [6]. Essential to successful vesicle formation is the proper recognition of membrane-bound receptor sorting signals by adaptor proteins. Specific examples of membrane-

bound receptors that contain adaptor protein-recognized sorting signals include the low density lipoprotein receptor, the transferin receptor, and the mannose-6-phosphate receptor [7]. Once the clathrin coated pit has been pinched from the plasma membrane of the donor organelle and entered the cytoplasm as a vesicle, clathrin and adaptor proteins disassemble from the vesicle and are recycled in the cytoplasm to form new coated pits and vesicles with specifically sorted luminal proteins and membrane-bound receptors at various cellular compartments. When clathrin and the adaptor proteins disassemble from the original vesicle in the cytoplasm, the vesicle continues to travel towards its appropriate intracellular destination [6]. Upon reaching its target organelle, the vesicle will fuse to the membrane of the acceptor organelle and donate its cargo proteins into the lumen of this organelle.

C. The Clathrin Triskelion

The clathrin molecule contains three heavy chains and three light chains. The three heavy chains converge at the center of the molecule to form a tri-pronged structure called a triskelion [8, 9]. While there is only one clathrin heavy chain (CHC) gene in most organisms [10], humans contain two paralogs of it [11]. In contrast, there are at least two paralogs for the clathrin light chain (CLC) gene expressed in bovine brain tissue. The alternative splicing of these genes results in the formation of longer proteins than are found in any other type of tissue [12]. The two light chain paralogs are interchangeable and may differ from each other only by the precise shape of the triskelion formed by the different chain-containing clathrin molecules [6].

D. Understanding the Coat: Layers, Function and Known Interactions

From Pearse's seminal work on the isolation and purification of clathrin coated vesicles, it became possible to examine the structure and function of coat components. The clathrin triskelion forms the outermost layer of the coat, encasing adaptor proteins that recognize and bind to membrane-bound protein receptors and their respective ligands. The clathrin layer is formed by interacting clathrin triskelions that create a dynamic cage in a characteristic lattice pattern [15] of interweaving hexagons and pentagons [1]. Inside of these clathrin cages, adaptor proteins interact directly with membrane-bound receptors found on donor organelle compartments. These receptors and their associated ligands become localized into clathrin coated pits (with inner adaptor and outer clathrin layers) before being pinched off of the plasma membrane and entering the cytoplasm as fully formed vesicles.

How are inner layer adaptors able to recognize specific membrane-bound receptors? This question can be answered by a thorough examination of the amino acid residues in the cytoplasmic regions of membrane-bound receptors. All receptors that have been successfully endocytosed contain either a tyrosine or di-leucine sorting motif on their cytoplasmic tails. These motifs have been hypothesized to interact directly with adaptor proteins as a means to ensure integration into coated vesicles [6, 16].

E. Adaptor Structure

Pearse and Bretscher first described adaptors in 1981 as molecules that facilitate proper sorting of membrane-bound receptors and ligands into clathrin coated vesicles [7]. Since then, a total of four types of adaptor proteins have been identified: AP-1, AP-2, AP-3 and AP-4 adaptor proteins. Each of these adaptor proteins has one β subunit and either a γ, α, δ or ε subunit (for AP-1 – AP-4, respectively). In addition to these large

subunits, each adaptor protein has a medium sized μ subunit and a small σ subunit [17]. While clathrin molecules have a triskelion structure, adaptor proteins have a core segment structure that attaches to appendage proteins, or "ears" [6, 18].

Of the four heterotetrameric adaptor proteins that have been identified, each has been found to localize at a different donor compartments and to target specific membrane proteins in vesicles destined for unique acceptor organelles. The AP-1 molecule participates in vesicle formation at the trans-Golgi network (TGN) and at the endosome, acting as a shuttle for cargo proteins between these two organelles. The AP-2 molecule localizes at the plasma membrane and targets proteins to the endosome, while AP-3 has been identified to form vesicles at the endosome and targets to lysosome-related organelles and synaptic vesicles [19, 20]. In our study, we will focus on AP-1, AP-2, and AP-3 interactions with clathrin, as well as participation of these adaptors in clathrin-dependent and independent trafficking pathways.

F. Adaptor Function

Adaptor proteins fulfill many roles within trafficking pathways. They are responsible for recruiting clathrin to sites of high protein concentration at various cellular compartments and also for directing mature vesicles to their appropriate destinations [21]. Adaptor proteins interact directly with specific motifs found on membrane-bound receptors, as well as with clathrin triskelions, acting as a critical link between clathrin and appropriate cargo proteins [6, 19].

Adaptor proteins also play a role in clathrin cage formation, as rates of cage production and precision of formation increases when adaptors are added into clathrin mixtures. While clathrin will self-assemble into cages in solution with magnesium and at

a pH of 6.5, this is largely contingent upon clathrin having a concentration level that is at least 30 ug/mL [9, 22]. Below this critical concentration, clathrin cannot assemble unless adaptors proteins are present. Cages created in the presence of adaptors are also more uniform in size than cages that are created by clathrin without adaptor proteins [23]. The specific nature of clathrin/adaptor interactions was first shown through three-dimensional maps generated from electron micrographs [24]. These maps showed that adaptor proteins interact not only with the clathrin coating, but also with the cytoplasmic regions of membrane-bound receptors inside of the clathrin cages [6] [**Figure 2**].

The specific intricacies of adaptor, clathrin, and cargo (membrane bound receptors and corresponding ligand) protein interactions are as follows. The AP-1 adaptor protein contains γ, β1, μ1, and σ1 subunits [25], of which the β1 binds to clathrin and the μ1 binds to cargo [26, 27]. While the AP-2 adaptor protein contains α, β2, μ2, and σ2 subunits [25], it has been substantiated that AP-2 binds to clathrin and cargos through relationships similar to those of AP-1; i.e. that the β2 subunit of AP-2 interacts with clathrin and its μ2 subunit interacts with cargoes [26, 27].

G. The Debate over AP-3

While the roles of AP-1 and AP-2 adaptor proteins in vesicle trafficking have been well established, AP-3's involvement in clathrin-dependent and clathrin-independent trafficking pathways is still under debate [**Figure 3**] [17]. To begin, several studies have shown that AP-3 interacts directly with clathrin and promotes its function in coat formation, supporting the hypothesis that AP-3 acts in clathrin-dependent trafficking pathways. A clathrin-binding sequence has been found in AP-3β3A and β3B subunits that is homologous to sequences found in the AP-1 and AP-2 β subunits [31, 32].

Additionally, *in vitro* studies have shown that AP-3 is able to co-assemble with clathrin and promote its recruitment to liposomes [31, 33]. Both of these studies provide support for the hypothesis that clathrin and AP-3 interact, although the specific nature of their interaction (and whether it is the same as AP-1 and AP-2/clathrin interactions) remains to be determined.

A second hypothesis concerning AP-3 participation in trafficking pathways holds that AP-3 promotes vesicle biogenesis independently from clathrin. Purified clathrin coated vesicles have been found to contain enriched quantities of AP-1 and AP-2 adaptors as compared to cell homogenate, which does not hold true for the AP-3 adaptor [28, 29]. This relative enrichment suggests that AP-1 and AP-2 bind to clathrin, and are purified along with the molecule through sub-cellular fractionation techniques while AP-3 acts independently and is therefore not enriched. Additional support for this hypothesis has been found through *in vitro* studies of microvesicle formation at the endosome, which requires AP-3 but not clathrin [30]. Ultimately, these results outline the possibility that AP-3 acts in clathrin-independent vesicle trafficking pathways.

A distinct third possibility is that AP-3 participates in clathrin-dependent as well as clathrin-independent trafficking pathways. Instead of considering AP-3 and clathrin as obligatory actors, it is possible that the two molecules may work independently from one another in overlapping pathways [17]. In support of this hypothesis, electron microscopy studies have found that only ~50% of all budding vesicle profiles containing AP-3 are also attached to clathrin [34, 35].

H. Significance of Clathrin Coated Vesicles to Cellular Transport and the Question Addressed by this Thesis

Proper cell function is achieved through the effective transport of molecules between the plasma membrane and intracellular organelles, and from donor to acceptor compartments. Vesicles assembled through clathrin-dependent mechanisms mediate these transport processes, selectively targeting proteins to particular cell domains and thereby creating cellular regions of specific molecular composition [36, 37]. An unresolved question is how clathrin regulates and specifies vesicle formation and composition in concert with adaptors in diverse sub-cellular locations such as the endosomes, Golgi apparatus, and plasma membrane. Currently, the model of clathrin coated vesicle formation holds that all types of adaptor proteins require clathrin for function. Additionally, this current model proposes that all types of adaptor proteins have similar mechanistic and kinetic interactions with clathrin. However, the precise nature of AP-3's interaction with clathrin in clathrin-dependent pathways, as well as its participation in clathrin-independent trafficking pathways, challenges this current model and will be examined over the course of this study.

A valuable strategy in the analysis of vesicle trafficking and clathrin/adaptor interactions is the direct visualization of clathrin molecules in intact cells. To achieve this goal, we have created a double-tagged clathrin molecule that possesses a red "mCherry" fluorescent protein and an oligomerization tag known as the FKBP binding domain. This domain binds to the drug AP20187, which results in nonfunctional clathrin. Thus, clathrin-dependent transport mechanisms are acutely halted. This rapid shut-down minimizes the possibility that membrane protein cargoes may be shuttled through the cell by alternative pathways, potentially altering adaptor concentration levels and functionality.

Only two published studies have reported that vesicle formation by the adaptors AP-2 and AP-1 is impaired after functional clathrin depletion [38, 39]. Here I have used biochemical approaches to analyze whether functional clathrin depletion affects AP-1, AP-2, and AP-3-dependent clathrin coated vesicle formation. My goal is to determine whether any differences exist between the three types of adaptor complexes and their interactions with clathrin. Additionally, I will examine the role that AP-3 plays in clathrin-independent trafficking pathways by considering whether AP-3 and clathrin directly interact. These findings might reveal a new regulatory mechanism of vesicle formation that operates in the interface between adaptors and clathrin.

Experimental Aims

A. Specific Objectives

1. To determine whether AP-3's interaction with clathrin in clathrin-dependent pathways is similar mechanistically and kinetically to AP-1 and AP-2/clathrin interactions. This will be achieved through biochemical analysis of adaptor protein concentrations in the clathrin coated vesicle cell fraction following an acute perturbation of clathrin.
2. To determine whether AP-3 is capable of interacting with clathrin, or if it acts only in clathrin-independent vesicle trafficking pathways. This will be achieved through an examination of the localization of AP-3 in donor and target organelle compartments, as well as the colocalization of AP-3 with clathrin triskelion components following an acute perturbation of clathrin.

B. Hypotheses

1. If all adaptors interact with clathrin in a similar manner, then all adaptors should respond similarly to acute perturbation of triskelia assembly. By contrast, if AP-3 has different kinetic or mechanistic interactions with clathrin than those of AP-1 and AP-2 with clathrin, then AP-3 will respond to an acute perturbation of clathrin in manner that is distinct from the other adaptor responses. I will test this hypothesis by comparing the relative enrichment of AP-3 to the other adaptor proteins in clathrin coated vesicle fractions following the functional depletion of clathrin triskelia through AP20187 treatment and mCherry-FKBP-CLC oligomerization.

2. If AP-3 interacts with clathrin triskelia containing clathrin light chain, my hypothesis predicts that inhibiting clathrin function in PC12 cells through AP20187 treatment will cause a subsequent increase in AP-3 clathrin colocalizations. This will be visualized through immunofluorescence microscopy experiments. Conversely, if AP-3 participates exclusively in trafficking pathways independent from clathrin, or if it is not capable of direct interaction with the clathrin triskelia, my hypothesis predicts that AP-3 will not colocalize with clathrin and its cellular localization will not be altered following AP20187 treatment.

Experimental Methods

A. PC12 Cell Line: Formation of Construct and Transfection

Formation of Construct:

The mCherry-FKBP-CLC construct was created from pmCherry and pEGFP-C1 vectors obtained from the Clontech Laboratories Inc. (1290 Terra Bella Ave., Mountain View, CA 94043 USA) and Enrique Rodriguez-Boulan, respectively [38]. The mCherry tag was initially amplified from the Clontech pmCherry vector using standard PCR techniques. NheI and BglII restriction sites were added to the mCherry tag through PCR, and this construct was ligated into a TOPO vector.

Separately, a HA-FKBP-LC construct was received from Enrique Rodriguez-Boulan. This construct, originally generated with FKBP vectors derived from ARIAD Pharmaceuticals, Inc. (26 Landsdowne Street, Cambridge, MA 02139-4234 USA), was contained within a pEGFP-C1 backbone. The HA fragment was eliminated from the construct by treatment with NheI and BglII restriction enzymes, which recognized and cut specific sites flanking the HA segment.

At this point, the TOPO vector was double digested with the NheI and BglII restriction enzymes, which released the mCherry tag from the rest of the TOPO plasmid. The mCherry tag was then ligated with the FKBP-LC domain into the pEGFP-C1 backbone, creating the final mCherry-FKBP-LC construct. This construct was transfected into PC12 cells according to the procedure below.

Transfection:

The day before transfection, cells were plated in antibiotic-free media and grown to 70-80% confluence. Two sets of tubes were prepared for each well to be transfected. One

hundred μL of Opti-MEM media was put in all of the tubes, while 4 μL of Liptofectamine was put into half of them. One half to 1 μg of plasmid DNA was put into the other half the tubes along with the Opti-MEM media. The solutions were incubated at room temperature for five minutes before the Lipofectamine solution was mixed into the DNA solution. Once combined, the solutions were incubated at room temperature for 20 minutes. Following incubation, 800 μL of Opti-MEM media was added to each Liptofectamine-DNA tube. The plates containing the confluent cells were removed from the incubator and washed twice with 2 mL of PBS and then with 2 mL of Opti-MEM. After these washes, the Liptofectamine-DNA solution was added to each well and the plates were returned to the incubator for four hours. Transfected cell lines were selected for by growth in antibiotic media containing 0.2 mg/mL of the neomycin antibiotic analog G418. Cells that had been successfully transfected were lifted from the wells and serially diluted on a 96 well plate. Colonies formed from these cell lines were made into stocks and their construct expression levels were compared through immunofluorescence. A cell line containing 100% of cells expressing the mCherry construct was stably maintained and used for all experiments.

B. Cell Culture

Cells were maintained in 15 cm plates in a 10% CO_2 humidified atmosphere at 37°. They were grown on DMEM medium containing 5% horse serum, 10% fetal bovine serum, 5 mL/500 mL penicillin and streptomycin, and 1 mL/500 mL G418 antibiotics. The cells were split weekly and used for clathrin coated vesicle isolation experiments between passages 12 and 20. They were grown to 95% confluence before these experiments and treated with 5% sodium butyrate 24 hours beforehand.

C. AP20187 Drug Treatment

Two hours prior to clathrin coated vesicle isolation experiments, plates were divided into two groups and treated either with ethanol (EtOH) or 50 nM AP20187 (obtained from ARIAD Pharmaceuticals, Inc.). These solutions were added directly to the cell media and the plates were placed back into a 10% CO_2 tank to incubate for two hours at 37°. The medium containing either EtOH or AP20187 was aspirated off at the beginning of the clathrin coated vesicle isolation experiment [**Figure 4**].

The AP20187 drug has been shown to functionally deplete clathrin within transfected cells where FKBP binding domains have been added to clathrin light chain triskelions. The drug interacts directly with two FKBP domains simultaneously, causing the oligomerization of clathrin triskelions [38, 39]. By disrupting the clathrin triskelion structure, the lattice-like clathrin cages required for vesicle formation are no longer able to form. Thus, through the AP20187 drug treatment we were able to render clathrin non-functional.

Ethanol was used as a vehicle control treatment in this experiment because it was also the vehicle for the AP20187 drug. Since AP20187 was dissolved within ethanol, by treating control group cells with a 50 nM concentration of ethanol we were eliminating ethanol as a variable from our experiment.

D. Clathrin Coated Vesicle Isolation

Clathrin coated vesicles were separated from other cellular compartments of PC12 cells through a process of sub-cellular fractionation. Following AP20187 and EtOH control treatment, plates were placed on ice and washed two times with PBS. Three mL of a 1X Buffer A solution (containing 19.52 g MES, 5 mL of 200 mM EGTA, 0.25 mL of

2M $MgCl_2$, and 100 mL MilliQ water) and Complete antiprotease mixture obtained from Roche Applied Science, Inc. (9115 Hague Road, P.O. Box 50414, Indianapolis, IN 46250-0414 USA) were added to each dish. The cells, detaching from the plates in this Buffer, were removed from their dishes and placed into two separate homogenizer tubes according to respective EtOH / AP20187 treatment groups. Cells were homogenized and the efficiency of homogenization was checked using Trypan Blue dye prior to the first centrifugation step. Fifty µL of both types of homogenate was saved at this point [**Figure 5**].

Following homogenization, cells were centrifuged at 17,000x g in a SS-34 rotor for 20 minutes. This produced the first pellet (P1) and supernatant (S1) fractions. Fifty µL of both types of S1 was saved at this point, and the pellet fractions were resuspended in 500 µL of 1X Buffer A before being saved as well. The S1 fractions were then centrifuged at 56,000x g in the Type 40 for 60 minutes, producing a second pellet (P2) and supernatant (S2). Fifty µL of both types of P2 and S2 fractions were saved. The second pellet fractions were resuspended in 750 mL of the 1X Buffer A and homogenized. After the resuspended pellet fractions were pipetted into centrifuge tubes, 1.25 mL of a D_2O solution was injected under the solutions. For the final step in this procedure, the P2 fractions and D_2O underlays were centrifuged at 116,000x g in the SW-55 rotor for 120 minutes. The final pellet obtained from this centrifugation step contained an enrichment of clathrin coated vesicles.

E. Protein Concentration Analysis

To determine the relative protein concentrations of each fraction from CCV preparations, a Bradford assay was preformed using a BioRad SmartSpec^{TM} Plus

Spectrophotometer. The respective protein concentrations obtained through spectrophotometry were used to determine the volume of sample loaded into each Criterion SDS-PAGE gel for Western blotting, to ensure that the same amount of protein (measured in micrograms) was added to each well from each fraction.

For spectrophotometry, two hundred μL of BioRad protein reagent (BioRad Protein Assay: Dye Reagent Concentrate) was added to 800 μL of water and mixed thoroughly before sample from each fraction was added in 2 μL increments. Absorbency readings were taken with the spectrophotometer following each 2 μL increment addition until a reading of absorbance > 0.1 was obtained. At this point, the amount of sample added and specific absorbance reading was recorded and used to calculate the protein concentration of each CCV fraction.

F. Coomassie Staining

Once the relative protein concentrations were obtained for each fraction, Coomassie stains were performed with Criterion SDS-PAGE gels for each CCV preparation to verify the accuracy and consistency of calculated protein concentrations before immunoblot analyses were performed. Because the Coomassie stain binds to protein bands based upon amount of protein present (independent of type), this enabled me to verify that the same overall protein concentration was loaded from each fraction into each well. Four-20% SDS-PAGE Tris-HCl Criterion gels were loaded with 10 μg of 4x sample buffer and 10 μg of each CCV fraction sample per lane and run at 120 mV until electrophoresis was determined to be complete by dye migration. The gel was then removed from its plastic casing and placed into a glass container along with 500 mL of a gel-fixing solution (50% v/v ethanol in water with 10% v/v acetic acid). The gel was rocked in this solution for an

hour and then washed overnight with a solution of 50% v/v methanol in water with 10% v/v acetic acid. To stain the gel, the gel was rocked with 400 mL of Coomassie Brilliant Blue R-250 Staining Solution obtained from BioRad Laboratories, Inc. (1000 Alfred Nobel Drive, Hercules, CA 94547 USA) for 30 minutes. It was destained with treatment of 300 mL of 50% v/v methanol in water with 10% v/v acetic acid for ~1 hour. The gel was stored in 5% v/v acetic acid until it was scanned into jpg files.

G. Immunoblot Analysis

The relative contributions of specific proteins in clathrin coated vesicle fractions were determined through standard Western blotting techniques. Ten µg of each fraction sample type was loaded with 10 µL 4x sample buffer into separate 30 µL wells in a 4-20% SDS-PAGE Tris-HCl Criterion gel. The gel was run at 120 mV until electrophoresis was determined to be complete by dye migration. The protein samples were then transferred to an Immobilon PDVF membrane by constant current application within a transfer apparatus for 65 minutes.

Once the proteins were successfully transferred onto Immobilon membranes, they were washed for 20 minutes in a 5% non-fat milk solution with TBST (0.05% Triton X-100, 25 mM TBS) and treated with primary antibodies overnight [**Table 1**]. After overnight treatment, membranes were washed three times with TBST for five minutes each time. Membranes were then treated with a 1/7000 dilution of the appropriate secondary antibody (either a mouse monoclonal or rabbit polyclonal conjugated with peroxidase) in TBST 5% non-fat milk for thirty minutes. After being incubated in secondary antibody, membranes were rinsed quickly with TBST to remove excess milk solution and washed three times with TBST for ten minutes each time.

At this point, protein-antibody complexes were visualized by Western Lighting™ ECL with Amerhsam Hyperfilm™ ECL high performance chemiluminescence film. Equal proportions of Western Lighting™ ECL oxidizing reagent and enhanced luminol reagent were combined on the Immobilon membrane and the following chemiluminescence reactions were exposed on Amerhsam Hyperfilm™ ECL film. Exposure lengths varied depending on the signal strength and were carried out to a range of intensities. Western blot exposures were scanned into jpg files that were analyzed for densitometry using the ImageJ technology (Image Processing and Analysis in Java, freeware from the National Institutes of Health, 9000 Rockville Pike, Bethesda, Maryland 20892 USA).

Primary Antibody	Concentration of Primary	Secondary Antibody	Primary Antibody and Provider Location
Clathrin Heavy Chain	1:1000	Mouse monoclonal	Becton-Dickinson Biosciences, Mountain View, CA
Clathrin Light Chain	1:5000	Rabbit polyclonal	Chemicon Millipore Corporation Billerica, MA
mCherry	1:1000	Rabbit polyclonal	Clontech Mountain View, CA
AP-1 γ	1:1000	Mouse monoclonal	Becton-Dickinson Biosciences, Mountain View, CA
AP-2 α	1:500	Mouse monoclonal	Becton-Dickinson Biosciences, Mountain View, CA
AP-3 β3	1:500	Rabbit polyclonal	Faundez Lab
AP-3 δ	1:500	Mouse monoclonal	Developmental Studies Hybridoma Bank University of Iowa
AP-3 σ3	1:1000	Rabbit polyclonal	Faundez Lab

AP-3 μ3	1:200	Rabbit polyclonal	Faundez Lab
PI4KinaseII-α	1:500	Rabbit polyclonal	Faundez Lab
SV2 (10H4)	1:500	Mouse monoclonal	Dr. R. Kelly University of California, San Francisco
Anti-synaptophysin (Sy-38)	1:2000	Mouse monoclonal	Chemicon Corporation Temecula, CA
VAMP2 (69.1)	1:2000	Mouse monoclonal	Synaptic Systems Corporation Göttingen, Germany
VAMP7-TI	1:750	Mouse monoclonal	Andrew Peden, University of Cambridge

Table 1: Primary Western Blot Antibody Concentrations, Corresponding Secondary Antibodies, and Primary Antibody Provider

H. Immunofluorescence Microscopy

The cells that were used for immunofluorescence microscopy were plated onto glass coverslips the same morning as the cells used in CCVs preparations were split a final time to ensure that the immunofluorescence images were directly comparative to the cells used in CCV preparations. Prior to plating the cells on the glass slides, the coverslips were treated with 90 μL of Matrigel. This was incubated on the slides for 20 minutes before the excess Matrigel was aspirated off and 500 μL of sterile DMEM media was added. PC12 cells were added in 1 μL increments to each well until 20% confluency was reached within the wells. The cells were incubated overnight in a 10% CO_2 atmosphere and then treated with either EtOH or 50 nM AP20187 for two hours.

To then prepare the slides for immunofluorescent microscopy, the plates were removed from the CO_2 incubator and immediately placed on an ice bath. The media was aspirated from the wells, and the slides were washed two times with 0.5 mL ice cold 1X

PBS containing 1mM $MgCl_2$ and 0.1mM $CaCl_2$. The cells were fixed by a 20 minute treatment with 0.25 mL ice cold 4% paraformaldehyde in 1X PBS solution. Following this treatment, the slides were washed two times with 0.5 mL 1X PBS solution. The cells were blocked and made permeable with 0.5 mL blocking solution (containing 2% BSA, 1% fish skin gelatin, 15% horse serum and 0.02% saponin in PBS) for 30 minutes at room temperature. Plates were then incubated with 0.25 mL/well of primary (1°) antibody [**Table 2**] in IF blocking solution for 30 minutes in a 37° bath. Following treatment with 1° antibody, plates were rinsed three times with IF blocking solution. They were then incubated with secondary (2°) antibodies obtained from the Invitrogen Corporation (5791 Van Allen Way, P.O. Box 6482 Carlsbad, CA 92008) in IF blocking solution for 30 minutes in a 37°C bath. Following treatment with 2° antibody, plates were rinsed twice with IF blocking solution and once with 1X PBS solution. Glass slips were then mounted onto glass slides using a small amount of Gelvatol and left to dry in a dark container overnight. Once dry, the slides were sealed with nail polish and stored in the dark at 4° until imaged.

Images were acquired with a Plan Apochromat 63x/1.4 oil DiC objective on a Axiovert100M microscope that was coupled with a HeNe1, Argon ion and Coherent Verdi pumped Ti:Saphire laser. The images were then processed with the MetaMorph software (version 3.0, Universal Imaging Corporation, 402 Boot Road, Downington, PA 19335 USA) [40].

Primary Antibody	Concentration of Primary	Secondary Antibody
Clathrin Heavy Chain	1:1000	Mouse Monoclonal IgG1 Alexa G-488 (green)
mCherry	1:500	Rabbit Polyclonal Alexa R-555 (red)
AP-3	1:100	Mouse Monoclonal IgG1 Alexa G-488 (green)

Table 2: Primary Immunofluorescence Antibody Concentrations and Corresponding Secondary Antibodies

Results

A. Effect of AP20187 on Protein Concentration in Clathrin Coated Vesicle Fractions:

Upon determining appropriate sample volumes, Coomassie stains were performed for each clathrin coated vesicle preparation to check the accuracy of protein concentrations and loading techniques [**Figure 6**]. For each CCV preparation, comparative protein concentrations were found for all of the sub-cellular fractions of EtOH and AP20187-treated sub-cellular fractions, as each lane retained similar amounts of Coomassie dye. A notable exception is lane 7 (AP20187-treated cell homogenate), where the relatively higher Coomassie staining intensity indicates a probable loading error. Nonetheless, clathrin heavy chain concentration (indicated by an arrow at the right of Fig. 5) was found to significantly decrease from EtOH (control, lanes 1-6) to AP20187-treated cells (lanes 7-12) despite the greater AP20187 homogenate concentration. Comparing the intensity of the Coomassie stained CHC bands from homogenate to CCV fractions for both EtOH and AP20187-treated cells shows the successful enrichment of the clathrin heavy chain through the process of sub-cellular fractionation. Similarly, comparing the intensity of the CHC band to other protein bands within the EtOH and AP20187 CCV fractions shows that the CHC band is the most prominent protein, and has thus been successfully enriched through the CCV preparation. Finally, a comparison of the CHC band between the EtOH and AP20187 CCV lanes (6 and 12) shows that the clathrin molecule was functionally inhibited by AP20187 drug treatment as CHC concentration decreases from EtOH to AP20187-treated cells, despite similar protein concentration levels overall.

B. Effect of AP20187 on Protein Content in Clathrin Coated Vesicle Fractions: Cargoes, Adaptor Proteins and Clathrin Cages

In order to determine the relative concentrations of clathrin molecules between EtOH and AP20187-treated CCV fractions, Western blots were probed for clathrin heavy chain, clathrin light chain, and mCherry-FKBP tagged CLC proteins [**Figure 7**]. Probing for these molecules tested for the presence of clathrin triskelia components, which were found to be enriched within CCV fractions (from homogenate fractions) for both EtOH and AP20187-treated cells. Notably, all three clathrin components decreased in concentration from EtOH to AP20187-treated cells. This result confirmed the ability of AP20187 drug treatment in rendering clathrin non-functional.

To assess the relative enrichment of adaptor proteins between EtOH And AP20187-treated CCV fractions, Western blots were probed for AP-1 γ, AP-2 α, and AP-3 δ proteins [**Figure 8]**. Concentration levels of AP-1 γ and AP-2 α decreased in CCV fractions from EtOH to AP20187-treated cells, while AP-3 δ became further enriched in AP20187-treated cells (compare lanes 6 and 12). These results support the hypothesis that AP-3 adaptor proteins are capable of acting in clathrin-independent trafficking pathways, or that they act in clathrin-dependent pathways with different kinetics than either AP-1 γ or AP-2 α adaptors. [**Figure 9**].

In order to determine the relative concentrations of CCV cargo proteins, Western blots were probed for PI4KinaseIIα, VAMP7-TI, VAMP2, Sphysin and SV2. As all of these membrane proteins are targeted to synaptic-like microvesicles, it was predicted that the concentrations of these cargoes would be reduced in CCVs following AP20187 addition [**Figure 10**]. As expected, a statistically significant decrease in concentration

was found for all types of cargo proteins from EtOH to AP20187-treated CCV fractions (compare lanes 6 and 12).

Immunoblots from three independent CCV preparations were scanned into jpg files and analyzed by densitometry. The difference in densitometry between EtOH and AP20187 CCV fractions were normalized to AP-1 γ and AP-2 α controls and analyzed with the Student-Newman-Keuls Test of Multiple Comparisons [**Figure 11**]. AP-3 β3, AP-3 δ, and AP-3 σ3 subunits were found to significantly increase in concentration from EtOH to AP20187 CCV fractions, while no significant difference in densitometry was found for the AP-3 μ3 subunit. All examined cargo proteins (PI4 Kinase IIα, VAMP7-TI, VAMP2, Sphysin and SV2) were found to significantly decrease in AP20187-treated cells. Since the cargo proteins entering the cell from the plasma membrane require interaction with AP-2/clathrin vesicles before entering AP-3/clathrin vesicles, this data fits into the hypothesis that AP-2 and AP-3 have different kinetic interactions with clathrin (specifically that AP-2/clathrin vesicles are depleted from the cell more quickly than AP-3/clathrin vesicles).

C. Effect of AP20187 on Clathrin Heavy Chain and mCherry Colocalization by Immunofluorescent Microscopy

The effect of AP20187 treatment on clathrin localization within cells was tested using immunofluorescent techniques and confocal microscopy [**Figure 12**]. Clathrin Heavy Chain was detected with the monoclonal antibody X22 followed by Alexa G-488 conjugated secondary antibodies and mCherry-FKBP-CLC was detected with anti-mCherry antibodies and Alexa R-555 conjugated secondary antibodies, so that any colocalization appears in yellow. The localization of CHC and mCherry was dramatically

altered by AP20187-treatment. In EtOH-treated control cells (Fig. 12, left panel), CHC and mCherry molecules colocalized throughout the cytoplasm, as well as in the perinuclear region. However, rendering the clathrin molecule non-functional eliminated the presence of CHC and mCherry in the cytoplasm, instead trapping the two molecules in the perinuclear region. This is seen by the presence of large yellow puncta surrounding the nuclear region (Fig. 12, right panel). The number and size of perinuclear puncta are far more pronounced in AP20187 then in EtOH-treated cells. Finally, the addition of AP20187 caused the median values of colocalization between CHC molecules and mCherry-FKBP-CLC domains to increase from ~60 to 70% [**Figure 14**].

D. Effect of AP20187 on CLC and AP-3 Colocalization in Immunoflourescent Microscopy

The effect of AP20187 treatment on the colocalization of AP-3 and mCherry- FKBP-CLC domains within cells was studied through immunofluorescent microscopy [**Figure 13**]. AP-3 δ was detected with the monoclonal antibody X22 followed by Alexa G-488 conjugated secondary antibodies, and mCherry-FKBP-CLC was detected with anti-mCherry antibodies and Alexa R-555 conjugated secondary antibodies, making points of colocalization yellow in color. Following AP20187 treatment, colocalization between the two types of molecules increased dramatically from median values of 5 to 20% colocalization [**Figure 14**]. The cellular distribution of AP-3 also changed, as the colocalized AP-3 and mCherry-FKBP-CLC molecules congregated in the perinuclear region. This large manifold increase in colocalization between AP-3 and mCherry is consistent with the prediction that at least some AP-3 proteins interact with clathrin. If this was not the case, an acute perturbation of clathrin would not affect AP-3's cellular

localization, or the colocalization of AP-3 and clathrin components. Ultimately, considering the biochemical analysis in light of the immunofluorescent microscopy data favors the hypothesis that AP-3 interacts in clathrin-dependent pathways with different kinetics than AP-1 or AP-2. A final revised model of AP-3 interaction in vesicle trafficking pathways based upon the biochemical and microscopy results is shown in **Figure 15**.

Discussion

The results of these biochemical and microscopy analyses lend greatest support to the hypothesis that AP-3 participates in clathrin-dependent pathways, but interacts with clathrin in a manner that is unique in kinetics from AP-1 and AP-2. According to this hypothesis, the enrichment of AP-3 in CCV fractions following drug treatment is really the result of a relative increase in concentration, as the other adaptors are depleted from the cell at a faster rate than AP-3. That is to say that the absolute amount of AP-3 interacting with clathrin in AP20187-treated cells does not actually increase from the amount of AP-3 interacting with clathrin in the vehicle control cells. Instead, clathrin coated vesicles interacting with AP-1 and AP-2 are depleted from the cell more quickly than those interacting with AP-3, so that after drug treatment AP-3 proteins comprise a greater percentage of the overall protein found in CCV fractions. Because proteins were loaded into lanes based upon concentration, not volume or type, this provides substantial support for the relative enrichment of AP-3 following drug treatment. It would be incredibly beneficial for future studies to be directed towards understanding the kinetics of AP-3/clathrin interactions. One relatively straight-forward way to do this would be through an increase in drug treatment time (to 4 or 5 hours of incubation prior to CCV isolation) followed by an examination of the relative protein concentrations. This would elucidate whether the difference between AP-3/clathrin interactions and AP-1 or AP-2/clathrin interactions is one of kinetics. This type of experiment would also refine the hypotheses concerning AP-3 participation in clathrin-dependent and independent pathways.

A distinct second possibility is that AP-3 is capable of participating in alternative trafficking pathways that do not require functional clathrin for successful generation and targeting of vesicles. One option is that AP-3 can interact with clathrin even when clathrin light chains are not contained in the clathrin triskelions, a possibility that has been suggested for endocytosis at the plasma membrane [41]. However, this view is controversial as absence of CLC alters endocytosis parameters [42], and I do not favor this hypothesis because my confocal immunofluorescence experiments indicate that perturbation of clathrin triskelia with recombinant CLC (mCherry-FKBP-CLC) has a dramatic effect on the sub-cellular distribution of clathrin and AP-3.

On the other hand, it is possible that AP-3 acts in trafficking pathways that are entirely independent from clathrin. This hypothesis has been supported by *in vitro* studies of a particular pathway in microvesicle formation at the endosome that requires AP-3 but not clathrin [30]. Examining the biochemical data from this hypothesis suggests that the relative enrichment of AP-3 in the CCV fraction of AP20187-treated cells corresponds to a greater number of vesicles being generated in an alternative pathway. However, the information gained from the microscopy studies that show an increased colocalization between AP-3 and mCherry-FKBP-CLC following drug treatment does not favor this claim. Further studies of AP-3 interactions with other coat proteins would be beneficial to strengthening the hypothesis that AP-3 acts in clathrin-independent pathways.

Ultimately, my data does not eliminate the possibility that both hypotheses are correct and AP-3 participates in slowly recycling clathrin-dependent routes, while also acting in alternative trafficking pathways that do not require functional clathrin [**Figure 15**]. These results point to a model of AP-3 vesicle formation and cargo transport where clathrin

triskelion interactions differ dramatically from AP-1 and AP-2 adaptor protein complexes. While the AP-1 and AP-2 complexes must bind to clathrin for successful formation of vesicles at donor compartments, my data strongly suggests that this is not the case for AP-3. Instead, I propose that AP-3 and clathrin are capable of interaction but participate mainly in partially overlapping pathways. A critical question in my future studies is to determine the stoichiometry of interaction between AP-3 and clathrin.

Acknowledgements

I would like to thank my advisor, Dr. Victor Faundez, for welcoming me into his laboratory and guiding me throughout the research and writing processes of this work. I have been inspired by his good nature and the genuine interest he has had in my project, and I have truly appreciated the opportunity to learn from his example. I would also like to express immense gratitude to Stephanie Zlatic, my day-to-day instructor and very patient mentor. I could not have completed this project without her involvement! Finally, I would like to thank all of the members of the Faundez lab, for they have been wonderful guides in the laboratory and helped spark in me a genuine love and respect for research. This work was funded in part by the Summer Undergraduate Research Experience (SURE) program at Emory.

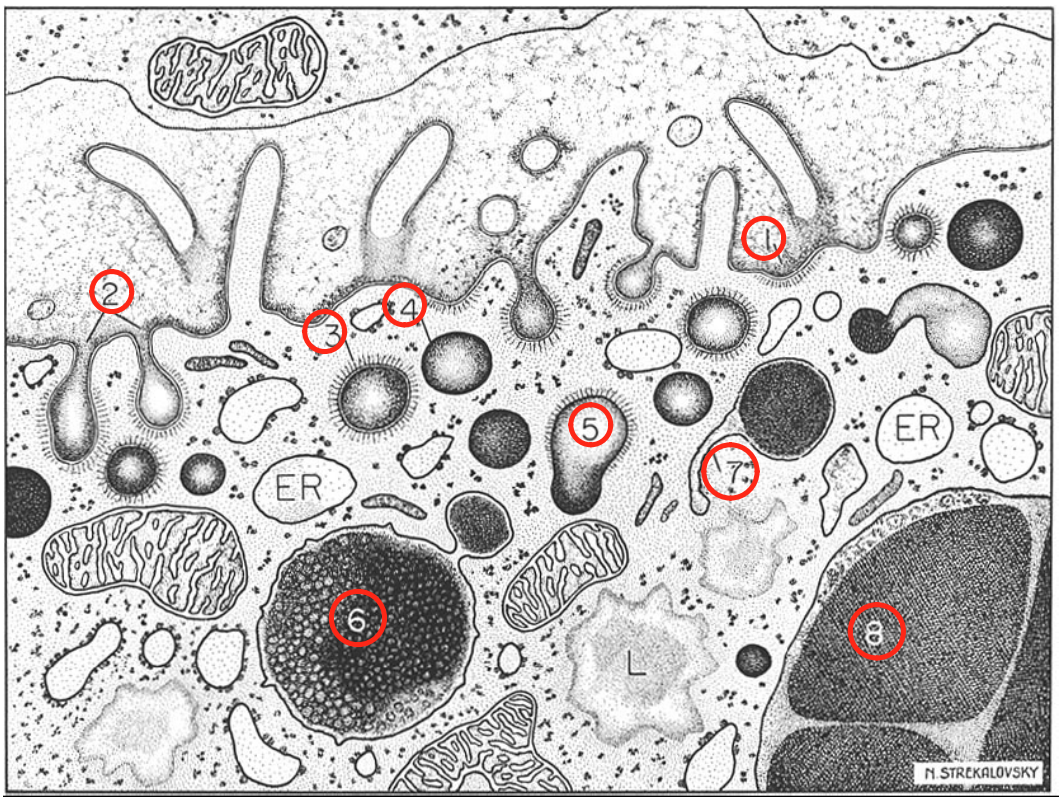

Figure 1: First schematic to depict coated pit and vesicle formation. At label (1) the formation of a coated pit is shown, as protein-covered plasma membrane buds into the intercellular space. Label (2) depicts mature pits pinching off of the membrane and entering the cytoplasm as coated vesicles (3). Imaged modified from [13].

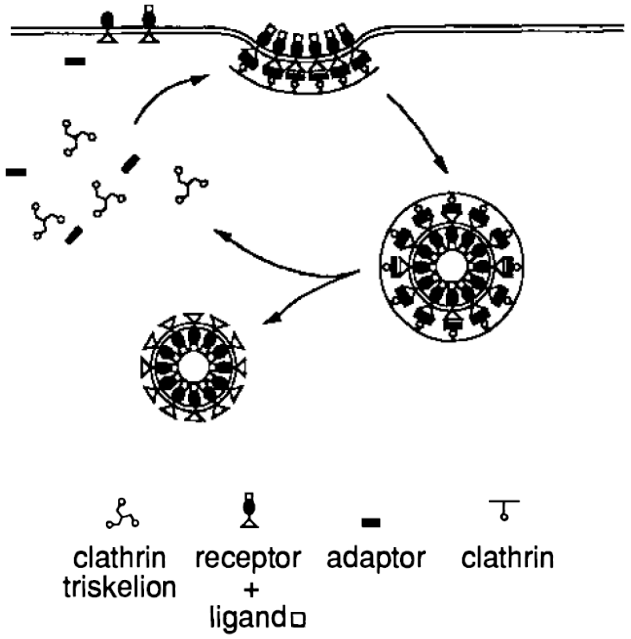

Figure 2: Schematic of the cycle of coated pit and clathrin vesicle formation. The different layers of the clathrin coat and adaptor interactions with clathrin and cargo proteins are shown here in the mature vesicle. Imaged obtained from [6].

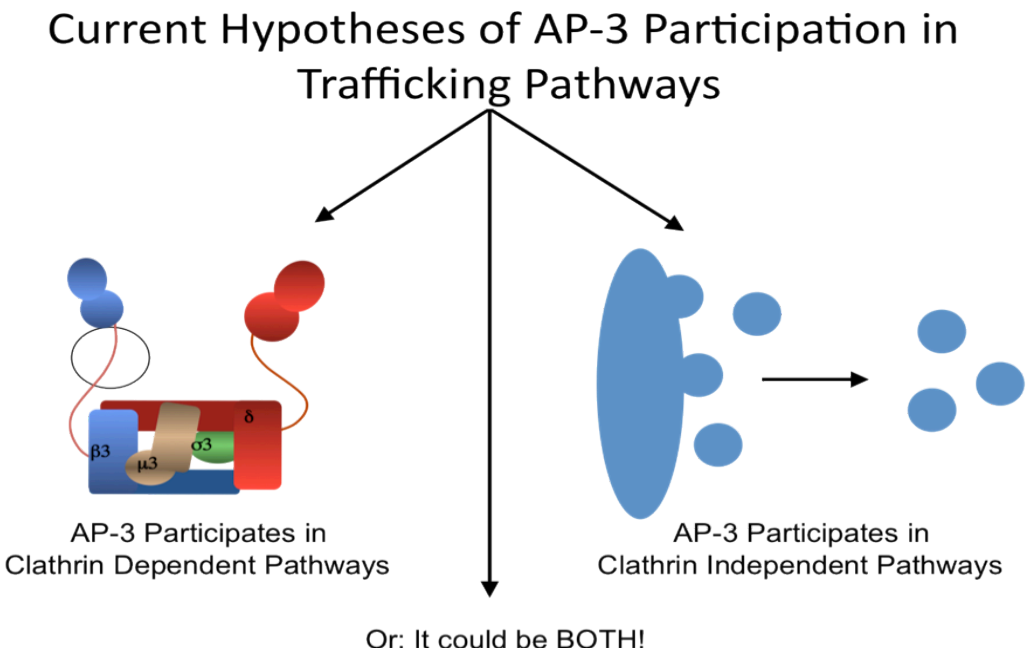

Figure 3: Current hypotheses concerning AP-3 participation in trafficking pathways. One proposal is that AP-3 acts only in clathrin-dependent pathways; a second proposal is that AP-3 participates entirely within clathrin-independent pathways, and a distinct third option is that AP-3 acts in both types of pathways. Our work will challenge these hypotheses concerning the role AP-3 plays in clathrin-dependent pathways, as well as its ability to function in clathrin-independent pathways.

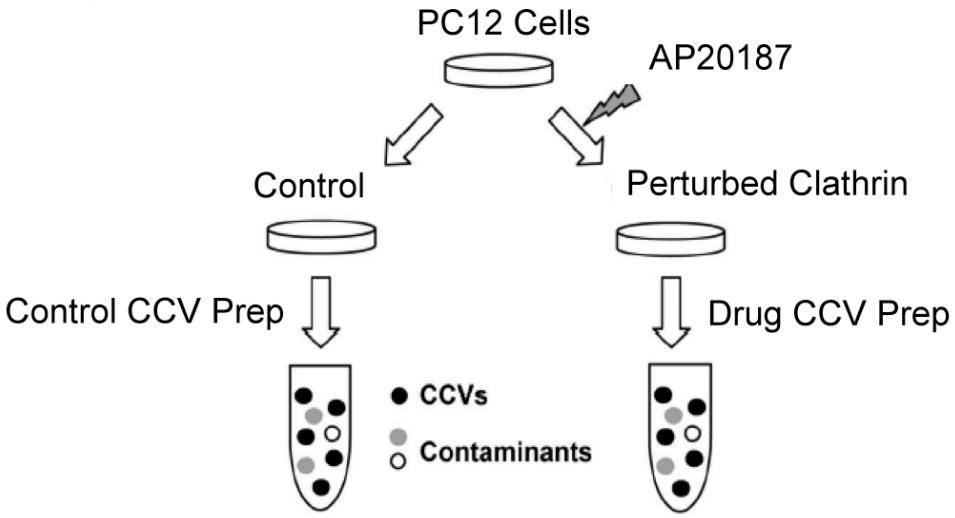

Figure 4: Schematic of EtOH and AP20187 treatment two hours prior to CCV preparations. Two hours prior to clathrin coated vesicle isolation experiments, plates were divided into two groups and treated either with ethanol (EtOH) or 50 nM AP20187. The EtOH-treated cells served as a control comparison group for the AP20187-treated cells, which contained clathrin molecules that had been rendered non-functional. The same two hour EtOH / AP20187 protocol was followed for cells then imaged through immunofluorescent microscopy.

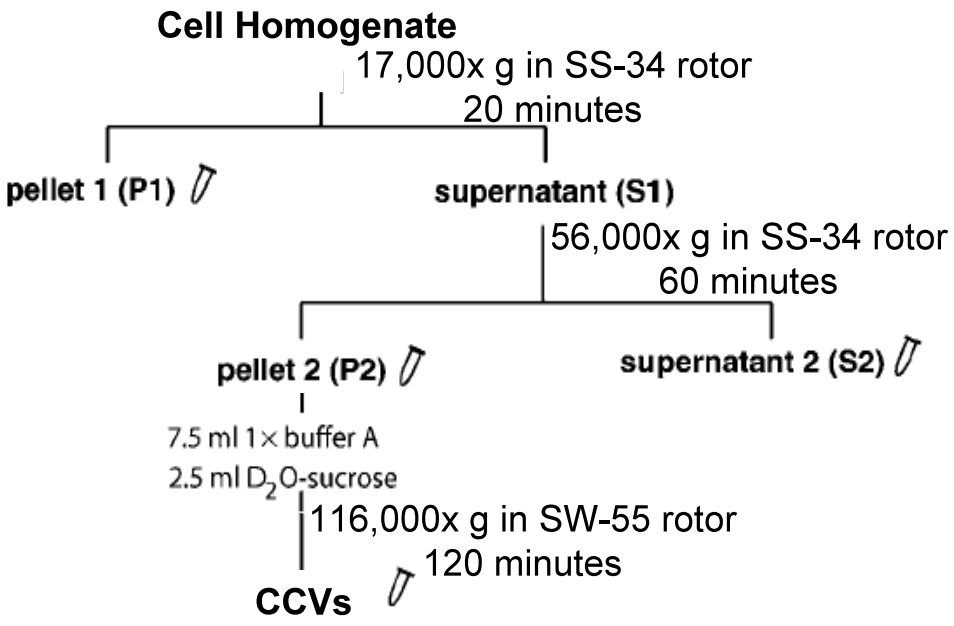

Figure 5: Clathrin coated vesicle sub-cellular fractionation procedure. Sub-cellular fractions P1, S1, P2, S2 and CCV samples were obtained through three independent centrifugation steps. Following initial homogenization, P1 and S1 were separated by a 20 minute centrifugation step at 17,000x g in a SS-34 rotor. P2 and S2 fractions were obtained from the S1 fraction by a 60 minute centrifugation step at 56,000x g again in a SS-34 rotor. The P2 fraction was then homogenized, put over a D_2O underlay and centrifuged for 120 minutes at 116,000x g in a SW-55 rotor to obtain the final CCV fraction.

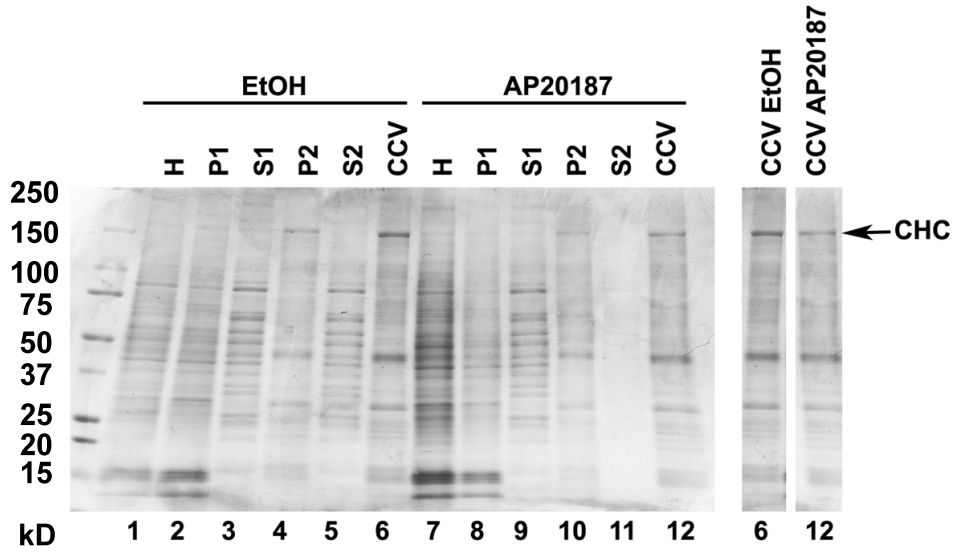

Figure 6: **Coomassie stain showing relative protein concentrations between sub-cellular fractions of CCV preparation**. The Coomassie staining intensity of gel lanes indicates that comparative amounts of protein were loaded in each lane, except for lane 7 (AP20187 homogenate) which was likely caused by a loading error. Comparing lanes 6 and 12 to 1 and 7, respectively, shows successful enrichment of Clathrin Heavy Chain from homogenate to CCV fraction for both EtOH and AP20187-treated cells. Additionally, examining the Clathrin Heavy Chain bands between lanes 6 and 12 reveals that CHC concentration decreases in AP20187-treated cells despite similar protein concentrations on an overall scale. Note: volume of sample loaded into each well was based upon protein concentration (obtained through spectrophotometry).

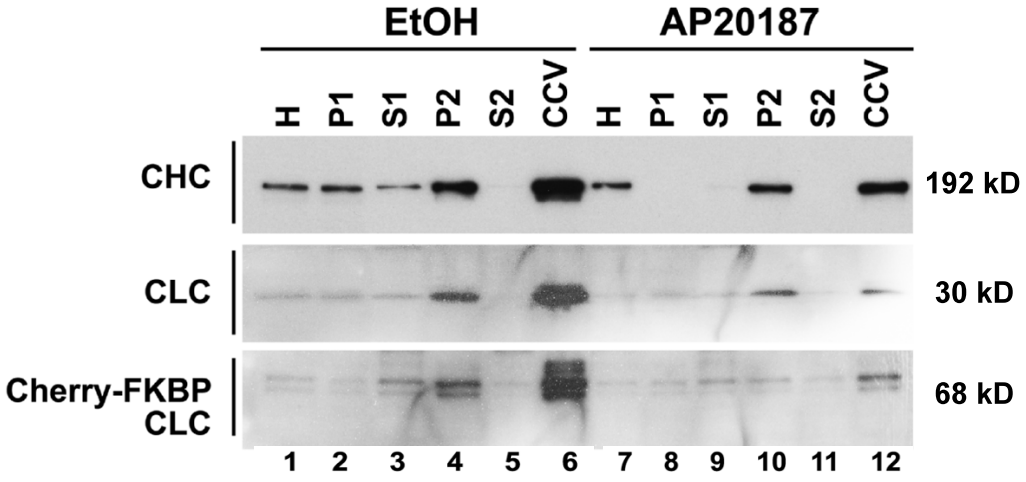

Figure 7: **Immunoblots of Clathrin Heavy Chain, Clathrin Light Chain, and mCherry-FKBP tagged CLC proteins for EtOH and AP20187 clathrin coated vesicle fractions.** These three components of clathrin triskelia were enriched in clathrin coated vesicle as compared to homogenate fractions for both EtOH and AP20187-treated cells. However, the enrichment in the CCV fraction for all of these markers decreased with AP20187 treatment (comparing lanes 6 and 12). Note: the loading controls for these Western blots are shown above (in **Figure 6**).

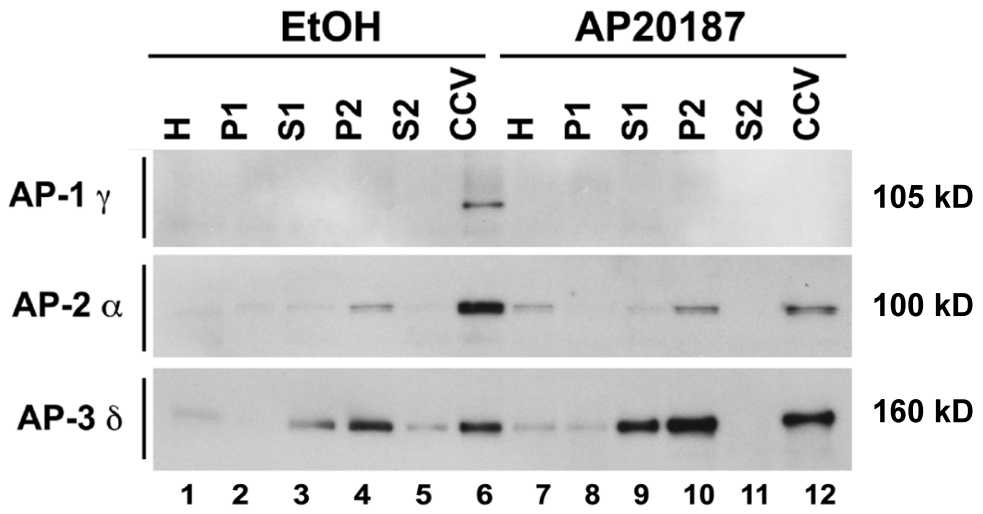

Figure 8: Immunoblots of AP-1 γ, AP-2 α, and AP-3 δ proteins for EtOH and AP20187 clathrin coated vesicle fractions. AP-1 γ and AP-2 α, as predicted by current notion, decrease in enrichment in clathrin coated vesicle fractions from EtOH to AP20187-treated cells (comparing lanes 6 and 12). However, AP-3 δ behaves differently from these other adaptor proteins, increasing in enrichment from EtOH (control) to AP20187-treated cells (again, comparing lanes 6 and 12). Note: the loading controls for these Western blots are shown above (in **Figure 6**).

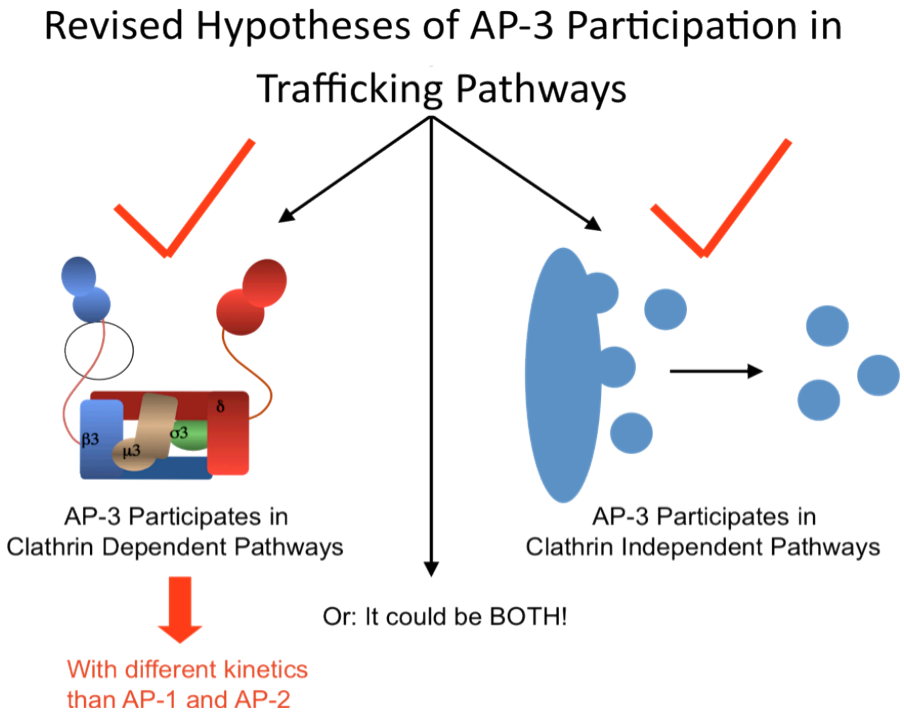

Figure 9: Revised hypotheses of AP-3 participation in trafficking pathways. The results obtained from the adaptor protein concentration analysis of the CCV fractions of EtOH and AP20187-treated cells supports the hypothesis that AP-3 participates in clathrin-dependent pathways with different kinetics than AP-1 and AP-2, as well as the hypothesis that AP-3 acts in clathrin-independent pathways.

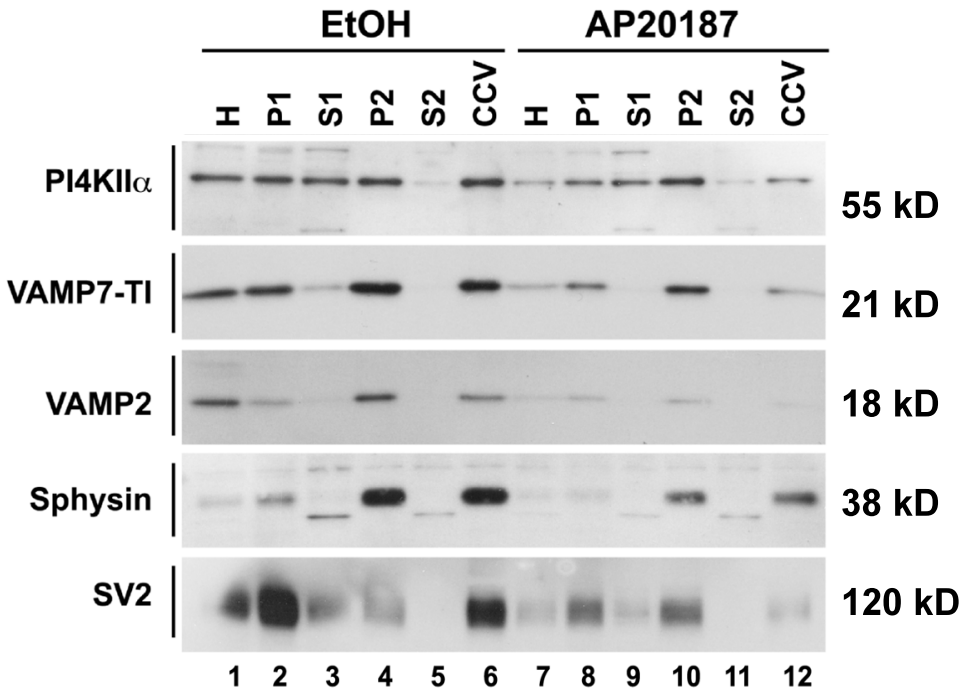

Figure 10: Immunoblots of PI4KinaseIIα, VAMP7-TI, VAMP2, Sphysin and SV2 cargo proteins for EtOH and AP20187 clathrin coated vesicle fractions. A statistically significant decrease in enrichment was found in the Clathrin Coated Vesicle fraction from EtOH to AP20187-treated cells for all types of cargo proteins examined. Note: the loading controls for these Western blots are shown above (in **Figure 6**).

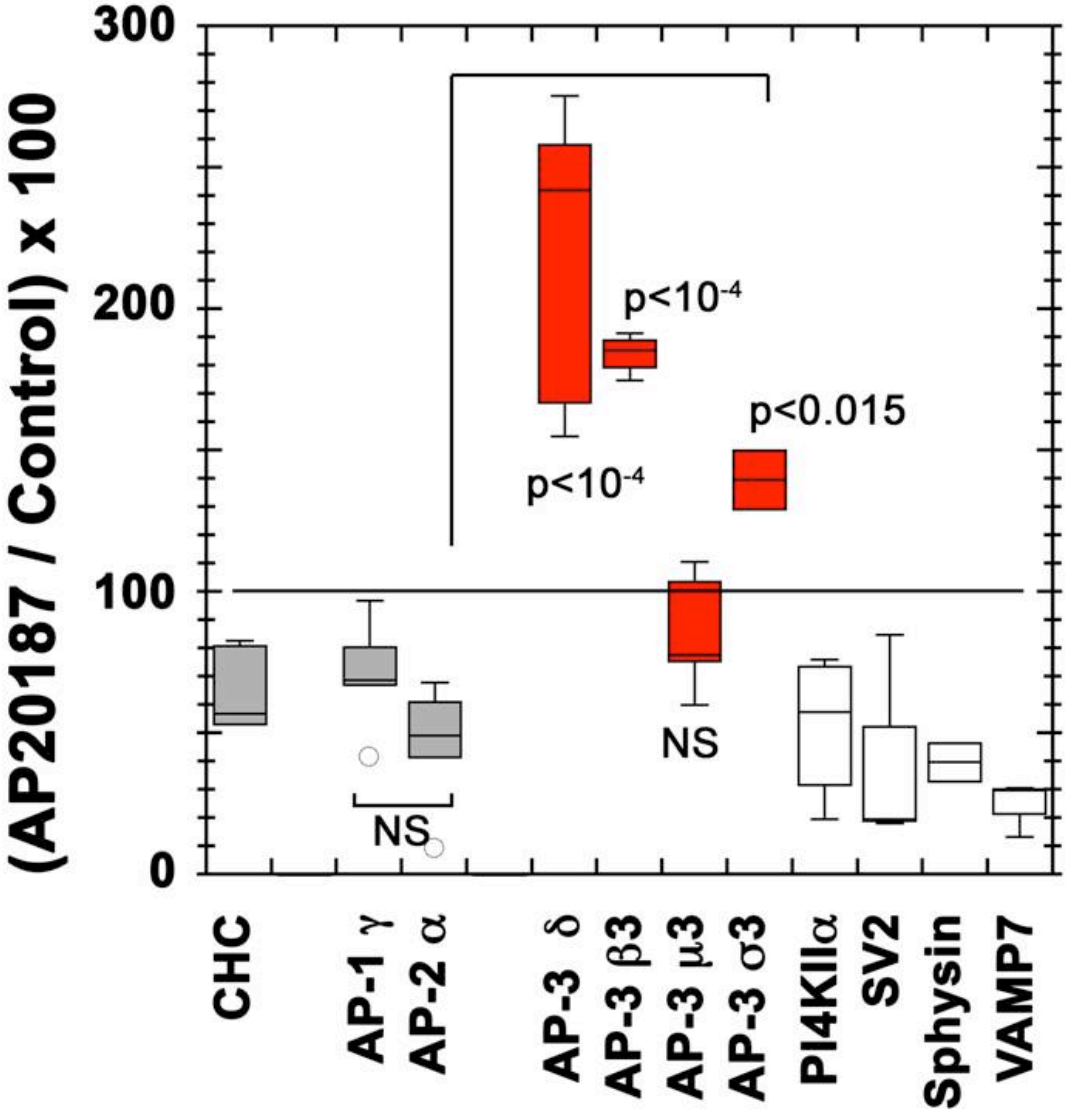

Figure 11: Student-Newman-Keuls Multiple Comparison of clathrin coated vesicle immunoblots (n=3). Immunoblots scanned into Jpg files and analyzed for densitometry were normalized to AP-1 γ and AP-2 α controls. Significant increases in densitometry were found in AP20187 Clathrin Coated Vesicle fractions (as compared to EtOH CCV fractions) for AP-3 β3, AP-3 δ, and AP-3 σ3 subunits. No significant difference in densitometry was found for the AP-3 μ3 subunit between AP20187 and EtOH CCV fractions when normalized to control. All examined cargo proteins (PI4KinaseIIα, SV2, Sphysin, and VAMP7) were found to significantly decrease in AP20187-treated cells.

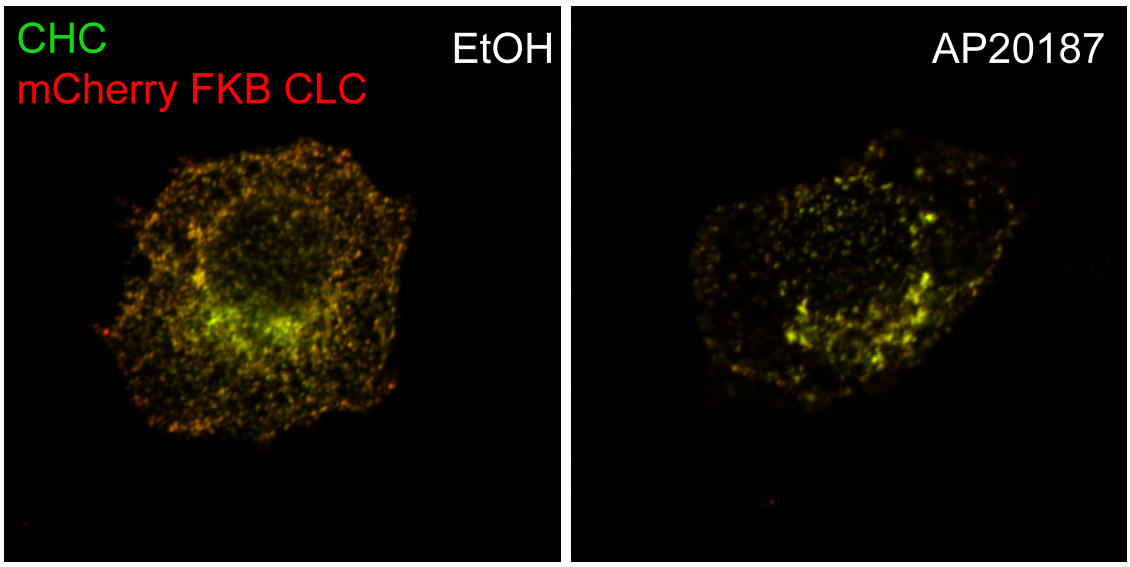

Figure 12: Immunofluorescence microscopy of CHC and mCherry in EtOH (left) and AP20187 (right) – treated cells, imaged with confocal microscope. Clathrin Heavy Chain is in green and mCherry-FKBP-CLC tag is in red fluorescence; points of localization of the two molecules are yellow in color. Cellular location of CHC and mCherry are dramatically altered by AP20187 treatment, shifting from the presence of both molecules on the plasma membrane and in the perinuclear region to an increased concentration at the perinuclear region and lack of presence in the cytoplasm. Colocalization of the two molecules was not significantly increased by drug treatment.

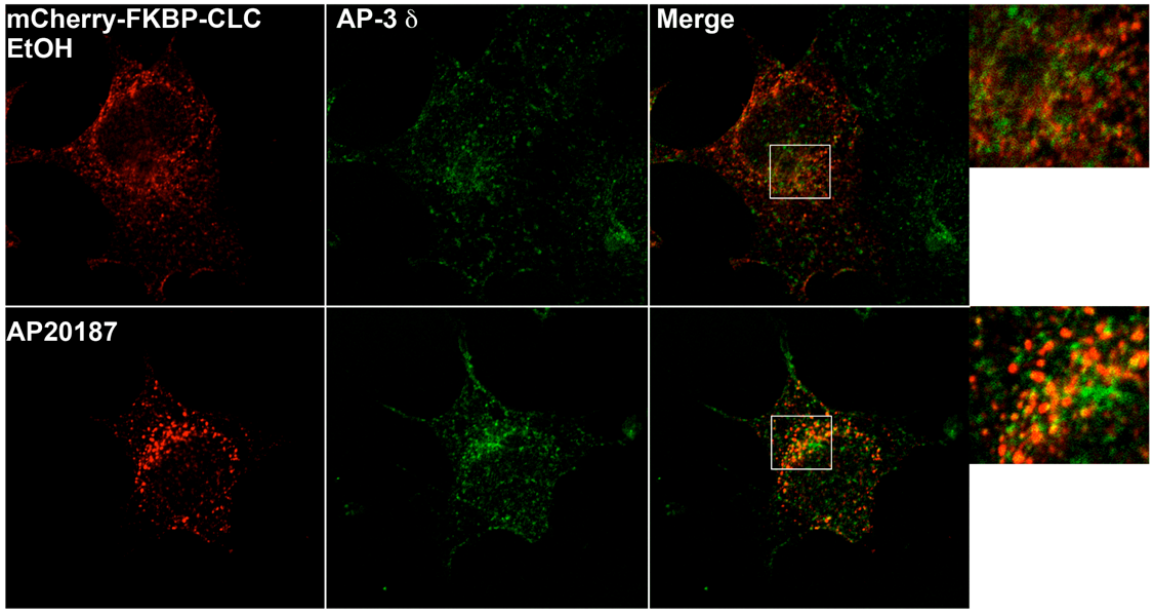

Figure 13: Immunofluorescence microscopy of AP-3 δ and mCherry in EtOH (above) and AP20187 (below)-treated cells, imaged with confocal microscope. AP-3 δ is in green and mCherry-FKBP-CLC tag is in red fluorescence; points of localization of the two molecules are yellow in color. Colocalization of AP-3 δ and mCherry increases following AP20187 treatment, and congregation of the two molecules increases in the perinuclear region. This suggests that AP-3 interacts directly with clathrin components in clathrin-dependent trafficking pathways. Image provided by Stephanie Zlatic.

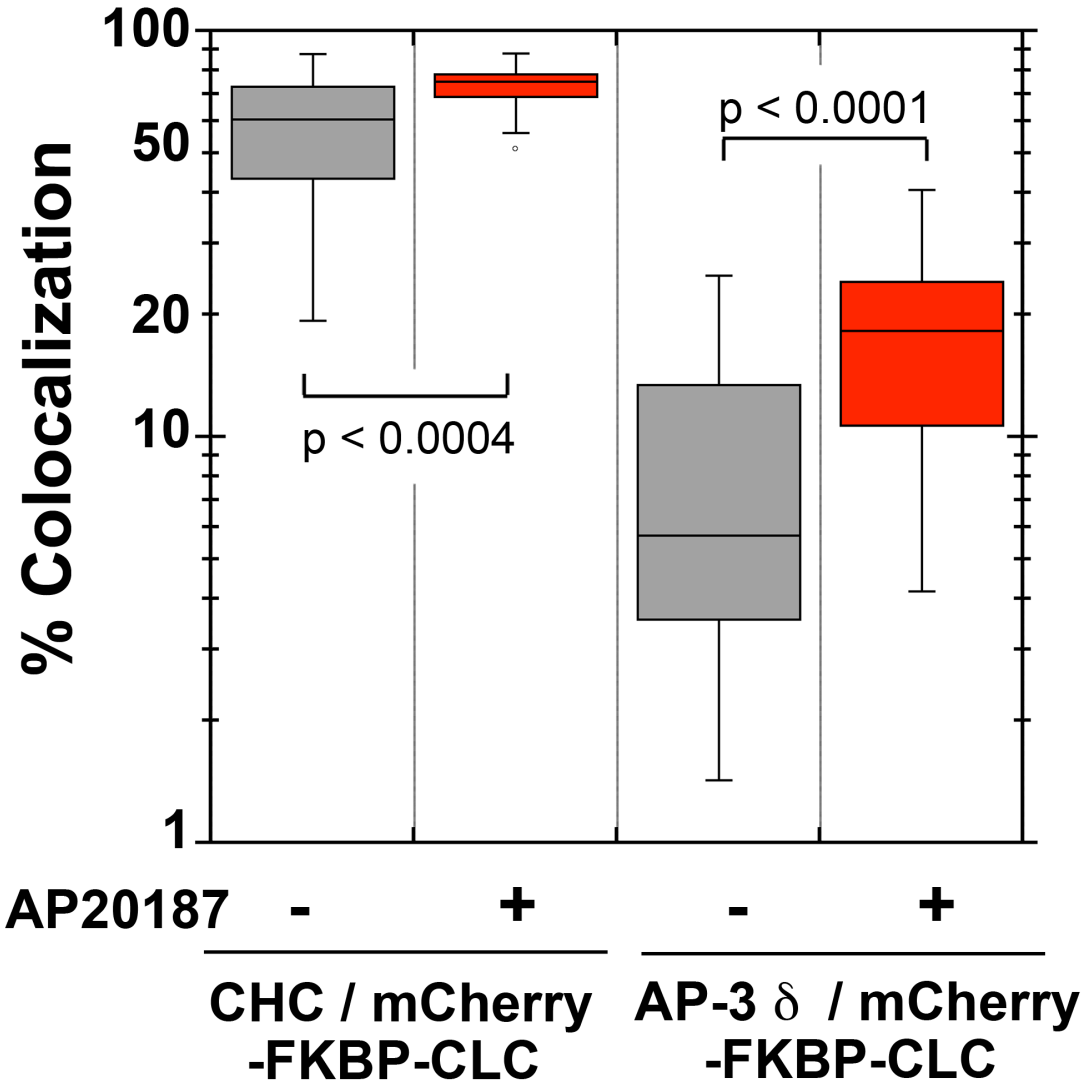

Figure 14: Wilcoxon-Mann-Whitney Rank Sum Test (non-parametric) of CHC/mCherry and AP-3 δ/mCherry colocalization of EtOH and AP20187-treated cells. Colocalization between CHC and mCherry following AP20187 treatment increased from median values of 60 to 70% colocalization. Even more dramatically, colocalization between AP-3 δ and mCherry following AP20187 treatment increased from median values of 5 to 20% colocalization. Note: Percentage of colocalization is shown on a logarithmic scale.

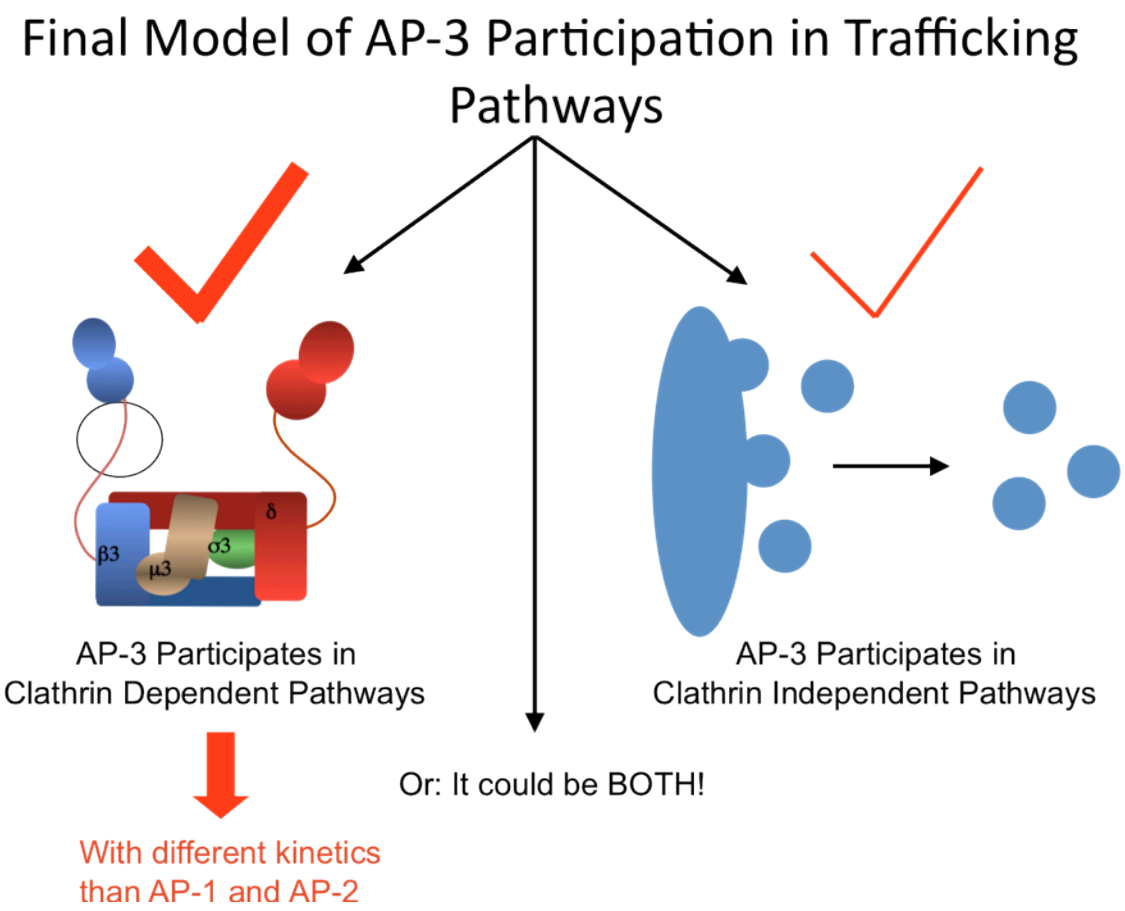

Figure 15: Final model of AP-3 participation in trafficking pathways. The manifold increase in colocalization between AP-3 and mCherry-FKBP-CLC molecules following AP20187 treatment lends support to the hypothesis that AP-3 participates in clathrin-dependent pathways with different kinetics of interaction than AP-1 or AP-2. While it does not eliminate the possibility that AP-3 participates in clathrin-independent pathways, it does not add any evidence to this claim. Thus, a consideration of both the biochemical and microscopy studies gives the greatest support to the first hypothesis.

References

1. Pearse, B.M., *Clathrin: a unique protein associated with intracellular transfer of membrane by coated vesicles.* Proc Natl Acad Sci U S A, 1976. 73(4): p. 1255-9.
2. Pearse, B.M., *Coated vesicles from pig brain: purification and biochemical characterization.* J Mol Biol, 1975. 97(1): p. 93-8.
3. Heerssen, H., R.D. Fetter, and G.W. Davis, *Clathrin dependence of synaptic-vesicle formation at the Drosophila neuromuscular junction.* Curr Biol, 2008. 18(6): p. 401-9.
4. Kasprowicz, J., et al., *Inactivation of clathrin heavy chain inhibits synaptic recycling but allows bulk membrane uptake.* J Cell Biol, 2008. 182(5): p. 1007-16.
5. Sato, K., et al., *Differential requirements for clathrin in receptor-mediated endocytosis and maintenance of synaptic vesicle pools.* Proc Natl Acad Sci U S A, 2009. 106(4): p. 1139-44.
6. Pearse, B.M. and M.S. Robinson, *Clathrin, adaptors, and sorting.* Annu Rev Cell Biol, 1990. 6: p. 151-71.
7. Pearse, B.M. and M.S. Bretscher, *Membrane recycling by coated vesicles.* Annu Rev Biochem, 1981. 50: p. 85-101.
8. Kirchhausen, T. and S.C. Harrison, *Protein organization in clathrin trimers.* Cell, 1981. 23(3): p. 755-61.
9. Ungewickell, E. and D. Branton, *Assembly units of clathrin coats.* Nature, 1981. 289(5796): p. 420-2.
10. Kirchhausen, T., et al., *Clathrin heavy chain: molecular cloning and complete primary structure.* Proc Natl Acad Sci U S A, 1987. 84(24): p. 8805-9.
11. Liu, S.H., et al., *A novel clathrin homolog that co-distributes with cytoskeletal components functions in the trans-Golgi network.* EMBO J, 2001. 20(1-2): p. 272-84.
12. Jackson, A.P., et al., *Clathrin light chains contain brain-specific insertion sequences and a region of homology with intermediate filaments.* Nature, 1987. 326(6109): p. 154-9.
13. Roth, T.F. and K.R. Porter, *Yolk Protein Uptake in the Oocyte of the Mosquito Aedes Aegypti. L.* J Cell Biol, 1964. 20: p. 313-32.
14. Kanaseki, T. and K. Kadota, *The "vesicle in a basket". A morphological study of the coated vesicle isolated from the nerve endings of the guinea pig brain, with special reference to the mechanism of membrane movements.* J Cell Biol, 1969. 42(1): p. 202-20.
15. Heuser, J., *Three-dimensional visualization of coated vesicle formation in fibroblasts.* J Cell Biol, 1980. 84(3): p. 560-83.
16. Bonifacino, J.S. and L.M. Traub, *Signals for sorting of transmembrane proteins to endosomes and lysosomes.* Annu Rev Biochem, 2003. 72: p. 395-447.
17. Peden, A.A., et al., *Assembly and function of AP-3 complexes in cells expressing mutant subunits.* J Cell Biol, 2002. 156(2): p. 327-36.
18. Owen, D.J., B.M. Collins, and P.R. Evans, *Adaptors for clathrin coats: structure and function.* Annu Rev Cell Dev Biol, 2004. 20: p. 153-91.

19. Knuehl, C. and F.M. Brodsky, *The long and short of adaptor appendages.* Nat Struct Biol, 2003. 10(8): p. 580-2.
20. Newell-Litwa, K., et al., *Neuronal and non-neuronal functions of the AP-3 sorting machinery.* J Cell Sci, 2007. 120(Pt 4): p. 531-41.
21. Kirchhausen, T., *Clathrin.* Annu Rev Biochem, 2000. 69: p. 699-727.
22. Crowther, R.A. and B.M. Pearse, *Assembly and packing of clathrin into coats.* J Cell Biol, 1981. 91(3 Pt 1): p. 790-7.
23. Zaremba, S. and J.H. Keen, *Assembly polypeptides from coated vesicles mediate reassembly of unique clathrin coats.* J Cell Biol, 1983. 97(5 Pt 1): p. 1339-47.
24. Vigers, G.P., R.A. Crowther, and B.M. Pearse, *Three-dimensional structure of clathrin cages in ice.* EMBO J, 1986. 5(3): p. 529-34.
25. Kirchhausen, T., *Adaptors for clathrin-mediated traffic.* Annu Rev Cell Dev Biol, 1999. 15: p. 705-32.
26. Gallusser, A. and T. Kirchhausen, *The beta 1 and beta 2 subunits of the AP complexes are the clathrin coat assembly components.* EMBO J, 1993. 12(13): p. 5237-44.
27. Ohno, H., et al., *Interaction of tyrosine-based sorting signals with clathrin-associated proteins.* Science, 1995. 269(5232): p. 1872-5.
28. Newman, L.S., et al., *Beta-NAP, a cerebellar degeneration antigen, is a neuron-specific vesicle coat protein.* Cell, 1995. 82(5): p. 773-83.
29. Simpson, F., et al., *A novel adaptor-related protein complex.* J Cell Biol, 1996. 133(4): p. 749-60.
30. Shi, G., et al., *Neuroendocrine synaptic vesicles are formed in vitro by both clathrin-dependent and clathrin-independent pathways.* J Cell Biol, 1998. 143(4): p. 947-55.
31. Dell'Angelica, E.C., et al., *Association of the AP-3 adaptor complex with clathrin.* Science, 1998. 280(5362): p. 431-4.
32. ter Haar, E., S.C. Harrison, and T. Kirchhausen, *Peptide-in-groove interactions link target proteins to the beta-propeller of clathrin.* Proc Natl Acad Sci U S A, 2000. 97(3): p. 1096-100.
33. Drake, M.T., Y. Zhu, and S. Kornfeld, *The assembly of AP-3 adaptor complex-containing clathrin-coated vesicles on synthetic liposomes.* Mol Biol Cell, 2000. 11(11): p. 3723-36.
34. Peden, A.A., et al., *Localization of the AP-3 adaptor complex defines a novel endosomal exit site for lysosomal membrane proteins.* J Cell Biol, 2004. 164(7): p. 1065-76.
35. Theos, A.C., et al., *Functions of adaptor protein (AP)-3 and AP-1 in tyrosinase sorting from endosomes to melanosomes.* Mol Biol Cell, 2005. 16(11): p. 5356-72.
36. Bonifacino, J.S. and B.S. Glick, *The mechanisms of vesicle budding and fusion.* Cell, 2004. 116(2): p. 153-66.
37. Conner, S.D. and S.L. Schmid, *Regulated portals of entry into the cell.* Nature, 2003. 422(6927): p. 37-44.
38. Deborde, S., et al., *Clathrin is a key regulator of basolateral polarity.* Nature, 2008. 452(7188): p. 719-23.

39. Moskowitz, H.S., et al., *Targeted chemical disruption of clathrin function in living cells.* Mol Biol Cell, 2003. 14(11): p. 4437-47.
40. Salazar, G., et al., *The zinc transporter ZnT3 interacts with AP-3 and it is preferentially targeted to a distinct synaptic vesicle subpopulation.* Mol Biol Cell, 2004. 15(2): p. 575-87.
41. Poupon, V., et al., *Clathrin light chains function in mannose phosphate receptor trafficking via regulation of actin assembly.* Proc Natl Acad Sci U S A, 2008. 105(1): p. 168-73.
42. Mettlen, M., et al., *Endocytic accessory proteins are functionally distinguished by their differential effects on the maturation of clathrin-coated pits.* Mol Biol Cell, 2009. 20(14): p. 3251-60.
43. Borner, G.H., et al., *Comparative proteomics of clathrin-coated vesicles.* J Cell Biol, 2006. 175(4): p. 571-8.